Classical Flight Dynamics of a Variable Forward-Sweep-Wing Aircraft

Brett A. Newman* and Robert L. Swaim†
Oklahoma State University, Stillwater, Oklahoma

The X-29 advanced technology demonstrator has established the design of forward-sweep wings. A conceivable variation of forward sweep is variable forward sweep. A variable forward-sweep configuration would likely offer higher performance levels than either forward sweep or variable sweep. The classical flight dynamics for such a configuration are determined and discussed. A classical aircraft stability analysis assuming rigid body, linearized dynamics, and no stability augmentation is used. Results indicated variable forward-sweep configurations can have less of a problem with excessive static margins than variable backward-sweep configurations. Wing location and center of gravity location changes due to variable forward sweep affect the stability derivatives consistently more than the wing shape changes due to variable forward sweep. The steady state trim condition and moments of inertia changes due to variable forward sweep and Mach number are small. The phugoid and roll modes experience the largest effects due to variable forward sweep and Mach number. The average handling quality levels experience no drastic changes due to variable forward sweep and Mach number.

Nomenclature

$[A_1]$ = longitudinal characteristic matrix
$[A_2]$ = lateral-directional characteristic matrix
b = wing span
$\bar{c}$ = wing mean chord
$C_{l_p}, C_{l_r}, C_{l_\beta}, C_{l_{\dot\beta}}$ = roll moment coefficient due to roll rate, yaw rate, sideslip angle, and sideslip angle rate, respectively
$C_{m_q}, C_{m_u}, C_{m_\alpha}, C_{m_{\dot\alpha}}$ = pitch moment coefficient due to pitch rate, forward speed, angle of attack, and angle of attack rate, respectively
$C_{n_p}, C_{n_r}, C_{n_\beta}, C_{n_{\dot\beta}}$ = yaw moment coefficient due to roll rate, yaw rate, sideslip angle, and sideslip angle rate, respectively
$C_{x_q}, C_{x_u}, C_{x_\alpha}, C_{x_{\dot\alpha}}$ = forward force coefficient due to pitch rate, forward speed, angle of attack, and angle of attack rate, respectively
$C_{y_p}, C_{y_r}, C_{y_\beta}, C_{y_{\dot\beta}}$ = side force coefficient due to roll rate, yaw rate, sideslip angle, and sideslip angle rate, respectively
$C_{z_q}, C_{z_u}, C_{z_\alpha}, C_{z_{\dot\alpha}}$ = downward force coefficient due to pitch rate, forward speed, angle of attack, and angle of attack rate, respectively
g = gravitational acceleration
$I_{xx}, I_{yy}, I_{zz},$ = moments of inertia for x, y, and z axes
I_{xz} = product of inertia for x and z axes
m = mass
M = Mach number
q = dynamic pressure
s = Laplacian variable
S = wing area
sm = static margin
u = forward speed
x = forward stability axis
$\bar{x}$ = forward design axis
y = side stability axis
$\bar{y}$ = side design axis
z = downward stability axis
$\bar{z}$ = downward design axis
α = angle of attack
β = sideslip angle
ζ = damping ratio
θ = pitch angle
Λ = wing leading edge sweep angle
τ = time constant
ϕ = roll angle
ψ = yaw angle
ω = natural frequency
% = (new value − old value)100/old value

Subscripts

AC = aerodynamic center
CG = center of gravity
DR = dutch-roll mode
P = phugoid mode
R = roll mode
S = spiral mode
SP = short period mode
1 = steady state

Introduction

THE X-29 advanced technology demonstrator has established the design of forward-sweep wings stiffened with layered composites to increase the wing structural divergence speed. A conceivable variation of forward sweep is the merging of forward sweep with variable sweep. Both configurations offer significant gains in performance relative to fixed backward-sweep configurations. The coupling of forward sweep with variable sweep would likely offer even higher performance levels. The objective of this study is to determine and discuss the classical flight dynamics for such a configuration.

Aircraft with variable backward sweep, such as the F-111, F-14, and B-1, have been designed with a minimum static margin at minimum sweep and subsonic speeds as shown in Fig. 1a.[1] Equation (1) defines static margin.

$$sm = \frac{\bar{x}_{CG} - \bar{x}_{AC}}{\bar{c}} \tag{1}$$

Note that low sweep is used at mid-subsonic speeds, mid sweep at intermediate speeds, and high sweep at low supersonic

Received Sept. 12, 1985; revision received Dec. 23, 1985.
*Master of Science Graduate. Student Member AIAA.
†Associate Dean and Professor. Associate Fellow AIAA.

speeds. The static margin increases with increasing sweep, assuming the aerodynamic center moves farther aft than the center of gravity. Supersonic speeds increase the static margin even more, due to the characteristic aft shift of the aerodynamic center. The static margin again increases with increasing sweep. An excessive static margin which restricts performance and maneuverability can occur at high sweep and supersonic speeds.[1,2]

Aircraft with variable forward sweep would logically be designed with a minimum static margin at maximum sweep and supersonic speeds as shown in Fig. 1b. The static margin increases with decreasing sweep, assuming the aerodynamic center moves farther aft than the center of gravity. This continues until subsonic speeds occur. Subsonic speeds decrease the static margin, due to the characteristic forward shift of the aerodynamic center. The static margin again increases with decreasing sweep. If this reduction in static margin due to Mach number is significant, aircraft using variable forward sweep will not be restrained as much by excessive static margins that typically occur with variable backward-sweep aircraft.

Aircraft stability derivatives, the steady state trim condition, and moments of inertia are also affected by variable forward sweep and Mach number. The effects from variable forward sweep are due to the changing wing shape, wing location, and center of gravity location. The effects from Mach number are due to the different aerodynamic behavior. As a result, the characteristic natural frequencies, damping ratios, and time constants are affected. These quantities determine the flight dynamics behavior.

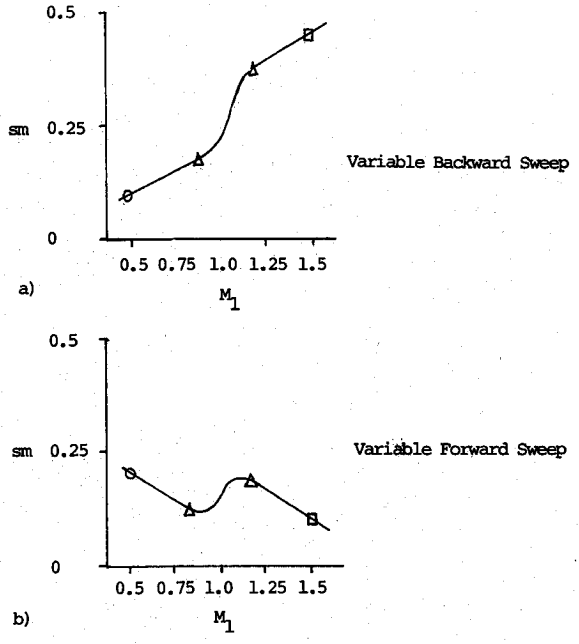

Fig. 1 Typical static margins as a function of sweep and Mach number.

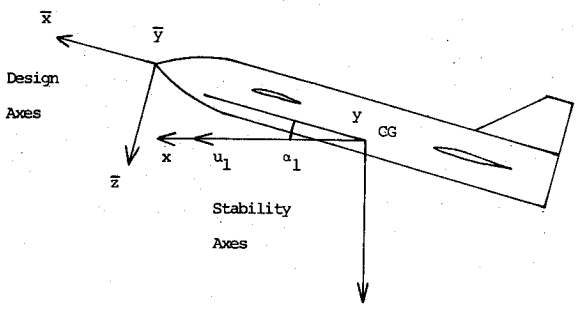

Fig. 2 Stability and design axes used in the study.

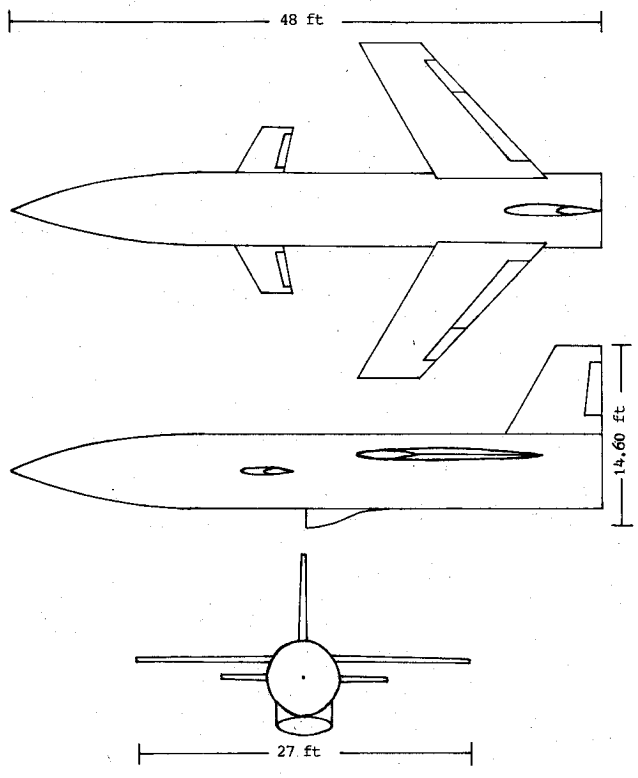

Fig. 3 Generic configuration at −30 deg sweep.

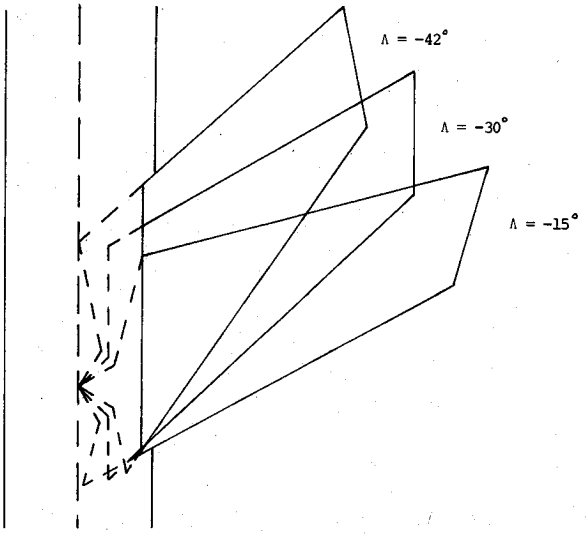

Fig. 4 Variable forward sweep wing geometry.

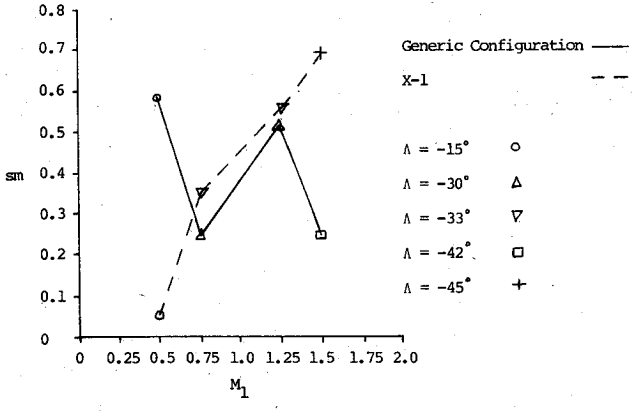

Fig. 5 Static margins as a function of sweep and Mach number for the generic configuration and the X-1 research aircraft model.[2]

Analysis and Generic Configuration

This study is a classical aircraft stability analysis.[3] Major assumptions include rigid body, linearized dynamics, and no stability augmentation. The uncoupled longitudinal and lateral-directional small perturbation equations of motion, written in the stability axes for a steady state rectilinear level flight condition, are used. Equations (2) and (3) are the characteristic matrices corresponding to the equations of motion with the longitudinal variables u, α, and θ and the lateral-directional variables β, ϕ, and ψ.

$$[A_1] = \begin{bmatrix} \frac{m}{q_1 S} - C_{x_u} & -C_{x_{\dot{\alpha}}} s - C_{x_\alpha} & -C_{x_q} + \frac{mg}{q_1 S} \\ -C_{z_u} & \left(\frac{mu_1}{q_1 S} - C_{z_{\dot{\alpha}}}\right) s - C_{z_\alpha} & -\left(\frac{mu_1}{q_1 S} + C_{z_q}\right) s \\ -C_{mu} & -C_{m_{\dot{\alpha}}} s - C_{m_\alpha} & \frac{I_{yy}}{q_1 S \bar{c}} s^2 - C_{m_q} s \end{bmatrix} \tag{2}$$

$$[A_2] = \begin{bmatrix} \left(\frac{mu_1}{q_1 S} - C_{y_{\dot{\beta}}}\right) s - C_{y_\beta} & -C_{y_p} s - \frac{mg}{q_1 S} & \left(\frac{mu_1}{q_1 S} - C_{y_r}\right) s \\ -C_{l_{\dot{\beta}}} s - C_{l_\beta} & \frac{I_{xx}}{q_1 sb} s^2 - C_{l_p} s & -\frac{I_{xz}}{q_1 Sb} s^2 - C_{l_r} s \\ -C_{n_{\dot{\beta}}} s - C_{n_\beta} & -\frac{I_{xz}}{q_1 Sb} s^2 - C_{n_p} s & \frac{I_{zz}}{q_1 Sb} s^2 - C_{n_r} s \end{bmatrix} \tag{3}$$

Figure 2 shows the coordinate systems used in the study. Stability derivatives are calculated from handbook methods.[3-5] Engineering English units are used throughout.

The generic configuration studied throughout is shown in Fig. 3. The aircraft uses a fixed centerline pivot, variable sweep wing shown in Fig. 4 with sweep angles ranging from -42 deg to -15 deg where negative denotes forward sweep. The configuration is similar to the unstable X-29 airframe. However, the generic configuration is designed stable. The design condition is a 0.25 static margin at -30 deg sweep, 0.75 Mach number, and 20,000 ft altitude. The generic configuration data are more fully presented in the Results section.

Results

The generic configuration's center of gravity location, aerodynamic center location, and wing mean chord for a typical sweep/Mach number profile are listed in Table 1. The static margins as determined from Table 1 for the generic configuration and Ref. 2 for the X-1 research aircraft model are shown in Fig. 5. The X-1 is the first variable-sweep model study in a wind tunnel. The X-1 uses a fixed centerline pivot, variable backward-sweep wing and suffers from excessive static margins at high sweep and supersonic speeds.

For the generic configuration, the static margin decreases with increasing sweep but increases with the aerodynamic center's aft shift due to Mach number. For the X-1, the static margin increases with increasing sweep and with the aerodynamic center's aft shift due to Mach number. The maximum static margin change for the generic configuration is 47% less than for the X-1. Consequently, variable forward-sweep configurations can have less of a problem with excessive static margins than variable backward-sweep configurations. This conclusion does not overlook that excessive static margins can be solved by outboard pivot locations or active controls, but rather indicates an inherent advantage of variable forward sweep.

The generic configuration data for the low condition (-15 deg sweep /0.5 Mach number), design condition (-30 deg sweep/0.75 Mach number), and high condition (-42 deg sweep/1.5 Mach number) of the sweep/Mach number profile used previously is listed in Tables 2-4. A positive time constant denotes a stable root. The handling quality levels as determined from the data in Tables 2-4 and Ref. 3 are listed in Tables 5-7. The generic configuration flight dynamics are discussed below, using the data listed in Tables 2-7.

The phugoid mode experiences the largest changes of the longitudinal modes due to the change from the design condition to the low condition. ω_P and ζ_P experience 40 and 61% reductions. C_{x_q}, C_{z_q}, C_{m_u}, C_{m_α}, and C_{m_q} experience the largest changes of the longitudinal stability derivatives ranging from 140 to 2100%. These stability derivatives are dependent upon the wing pitch moment arm; consequently, the large changes can be expected. It is surprising the short period mode is not affected more by the change from the design condition to the low condition, since so many key longitudinal stability derivatives are affected. The longitudinal handling-quality levels are not affected by the change from the design condition to the low condition, with a level 1.7 average for both conditions.

The dutch-roll mode experiences the largest changes of the lateral-directional modes due to the change from the design condition to the low condition. ω_{DR} experiences a 40% reduction. C_{l_p} and C_{n_p} experience the largest changes of the lateral-directional stability derivatives, 87 and 63%. These stability derivatives are dependent upon the wing roll and yaw moment arms and typically have wing contributions of equal or greater importance than the vertical fin contributions. Consequently, the large changes can be expected. It is surprising the roll mode is not affected more by the change from the design condition to the low condition since C_{l_p} is affected. The lateral-directional handling-quality levels are not affected by the change from the design condition to the low condition, with a level 1.3 average for both conditions.

The short period and phugoid modes both experience considerable changes due to the change from the design condition to the high condition. ω_{SP} and ζ_{SP} experience a 30% increase and 41% decrease. The phugoid mode changes to a pair of purely exponential modes, one stable and one unstable. C_{x_u}, C_{x_α}, and C_{z_u}, which do not depend upon the wing pitch moment arm, experience the largest changes of the longitudinal stability derivatives, 79%, 80%, and 98%. Most of the stability derivaties that depend upon the wing pitch moment arm experience smaller changes. Apparently, the wing pitch mo-

Table 1 Center of gravity location, aerodynamic center location, and wing mean chord as a function of sweep and Mach number for the generic configuration

$\Lambda - 15$ deg/$M_1 = 0.5$	$\Lambda = -30$ deg/$M_1 = 0.75$	$\Lambda = -30$ deg/$M_1 = 1.25$	$\Lambda = -42$ deg/$M_1 = 1.5$
$\bar{x}_{CG} = -26.86$[a]	$\bar{x}_{CG} = -26.55$	$\bar{x}_{CG} = -26.55$	$\bar{x}_{CG} = -26.34$
$\bar{y}_{CG} = 0$	$\bar{y}_{CG} = 0$	$\bar{y}_{CG} = 0$	$\bar{y}_{CG} = 0$
$\bar{z}_{CG} = -0.3281$	$\bar{z}_{CG} = -0.3281$	$\bar{z}_{CG} = -0.3281$	$\bar{z}_{CG} = -0.3281$
$\bar{x}_{AC} = -30.71$	$\bar{x}_{AC} = -28.46$	$\bar{x}_{AC} = -30.52$	$\bar{x}_{AC} = -28.64$
$\bar{c} = 6.618$	$\bar{c} = 7.684$	$\bar{c} = 7.684$	$\bar{c} = 9.390$

[a] All measurements in ft.

Table 2 Generic configuration data at the low condition

$\Lambda = -15$ deg	$M_1 = 0.5$	$q_1 = 172.4$ lbf/ft^2
$u_1 = 519.1$ ft/s	$\alpha_1 = 5.070$ deg	$\theta_1 = 0$ deg
$\beta_1 = 0$ deg	$\phi_1 = 0$ deg	$\psi_1 = 0$ deg
$S = 200.3$ ft^2	$\bar{c} = 6.618$ ft	$b = 31.39$ ft
$m = 1.984 \times 10^4$ lbm	$I_{xx} = 1.082 \times 10^6$ lbm ft^2	$I_{yy} = 1.750 \times 10^6$ lbm ft^2
$I_{zz} = 3.695 \times 10^6$ lbm ft^2	$I_{xz} = -2.297 \times 10^5$ lbm ft^2	$g = 32.18$ ft/s^2
$C_{x_u} = -3.667 \times 10^{-4}$ s/ft	$C_{z_u} = -1.859 \times 10^{-3}$ s/ft	$C_{m_u} = -7.702 \times 10^{-4}$ s/ft
$C_{x_\alpha} = -2.615 \times 10^{-1}$ 1/rad	$C_{z_\alpha} = -4.793 \times 10^{0}$ 1/rad	$C_{m_\alpha} = -2.711 \times 10^{0}$ 1/rad
$C_{x_{\dot\alpha}} = -5.190 \times 10^{-4}$ s/rad	$C_{z_{\dot\alpha}} = -1.114 \times 10^{-2}$ s/rad	$C_{m_{\dot\alpha}} = -1.461 \times 10^{-2}$ s/rad
$C_{x_q} = -1.875 \times 10^{-3}$ s/rad	$C_{z_q} = -3.466 \times 10^{-2}$ s/rad	$C_{m_q} = -1.255 \times 10^{-1}$ s/rad
$C_{y_\beta} = -8.090 \times 10^{-1}$ 1/rad	$C_{l_\beta} = -7.216 \times 10^{-2}$ 1/rad	$C_{n_\beta} = 9.967 \times 10^{-2}$ 1/rad
$C_{y_{\dot\beta}} = -3.567 \times 10^{-3}$ s/rad	$C_{l_{\dot\beta}} = -4.868 \times 10^{-4}$ s/rad	$C_{n_{\dot\beta}} = 1.953 \times 10^{-3}$ s/rad
$C_{y_p} = -7.874 \times 10^{-3}$ s/rad	$C_{l_p} = -1.199 \times 10^{-2}$ s/rad	$C_{n_p} = 2.743 \times 10^{-3}$ s/rad
$C_{y_r} = 5.599 \times 10^{-3}$ s/rad	$C_{l_r} = 2.046 \times 10^{-3}$ s/rad	$C_{n_r} = -1.546 \times 10^{-2}$ s/rad
$\omega_{SP} = 3.402$ rad/s	$\zeta_{SP} = 0.1644$	
$\omega_P = 0.04125$ rad/s	$\zeta_P = 0.08819$	
$\omega_{DR} = 1.046$ rad/s	$\zeta_{DR} = 0.1097$	
$\tau_R = 2.597$ s	$\tau_S = 24.20$ s	

Table 3 Generic configuration data at the design condition

$\Lambda = -30$ deg	$M_1 = 0.75$	$q_1 = 387.8$ lbf/ft^2
$u_1 = 778.6$ ft/s	$\alpha_1 = 3.358$ deg	$\theta_1 = 0$ deg
$\beta_1 = 0$ deg	$\phi_1 = 0$ deg	$\psi_1 = 0$ deg
$S = 200$ ft^2	$\bar{c} = 7.684$ ft	$b = 27$ ft
$m = 1.984 \times 10^4$	$I_{xx} = 1.005 \times 10^6$ lbm ft^2	$I_{yy} = 1.637 \times 10^6$ lbm ft^2
$I_{zz} = 3.527 \times 10^6$ lbm ft^2	$I_{xz} = -1.516 \times 10^5$ lbm ft^2	$g = 32.18$ ft/s^2
$C_{x_u} = -2.677 \times 10^{-4}$ s/ft	$C_{z_u} = -1.085 \times 10^{-3}$ s/ft	$C_{m_u} = -3.509 \times 10^{-5}$ s/ft
$C_{x_\alpha} = -1.876 \times 10^{-1}$ 1/rad	$C_{z_\alpha} = -4.369 \times 10^{0}$ 1/rad	$C_{m_\alpha} = -1.048 \times 10^{0}$ 1/rad
$C_{x_{\dot\alpha}} = -1.835 \times 10^{-4}$ s/rad	$C_{z_{\dot\alpha}} = -5.556 \times 10^{-3}$ s/rad	$C_{m_{\dot\alpha}} = -5.071 \times 10^{-3}$ s/rad
$C_{x_q} = -4.094 \times 10^{-4}$ s/rad	$C_{z_q} = -1.022 \times 10^{-2}$ s/rad	$C_{m_q} = -5.173 \times 10^{-2}$ s/rad
$C_{y_\beta} = -8.457 \times 10^{-1}$ 1/rad	$C_{l_\beta} = -9.298 \times 10^{-2}$ 1/rad	$C_{n_\beta} = 1.454 \times 10^{-1}$ 1/rad
$C_{y_{\dot\beta}} = -2.550 \times 10^{-3}$ s/rad	$C_{l_{\dot\beta}} = -4.501 \times 10^{-4}$ s/rad	$C_{n_{\dot\beta}} = 1.637 \times 10^{-3}$ s/rad
$C_{y_p} = -5.519 \times 10^{-3}$ s/rad	$C_{l_p} = -6.403 \times 10^{-3}$ s/rad	$C_{n_p} = 1.687 \times 10^{-3}$ s/rad
$C_{y_r} = 4.833 \times 10^{-3}$ s/rad	$C_{l_r} = 2.251 \times 10^{-3}$ s/rad	$C_{n_r} = -1.253 \times 10^{-2}$ s/rad
$\omega_{SP} = 3.559$ rad/s	$\zeta_{SP} = 0.1929$	
$\omega_P = 0.06880$ rad/s	$\zeta_P = 0.2270$	
$\omega_{DR} = 1.751$ rad/s	$\zeta_{DR} = 0.1246$	
$\tau_R = 2.637$ s	$\tau_S = 26.03$ s	

Table 4 Generic configuration data at the high condition

$\Lambda = -42$ deg	$M_1 = 1.5$	$q_1 = 587.9$ lbf/ft^2
$u_1 = 1{,}452$ ft/s	$\alpha_1 = 2.762$ deg	$\theta_1 = 0$ deg
$\beta_1 = 0$ deg	$\phi_1 = 0$ deg	$\psi_1 = 0$ deg
$S = 200.4$ ft^2	$\bar{c} = 9.390$ ft	$b = 22.14$ ft
$m = 1.984 \times 10^4$ lbm ft^2	$I_{xx} = 9.424 \times 10^5$ lbm ft^2	$I_{yy} = 1.574 \times 10^6$ lbm ft^2
$I_{zz} = 3.408 \times 10^6$ lbm ft^2	$I_{xz} = -1.270 \times 10^5$ lbm ft^2	$g = 32.18$ ft/s^2
$C_{x_u} = -5.568 \times 10^{-5}$ s/ft	$C_{z_u} = -2.468 \times 10^{-5}$ s/ft	$C_{m_u} = -1.857 \times 10^{-5}$ s/ft
$C_{x_\alpha} = -3.378 \times 10^{-1}$ 1/rad	$C_{z_\alpha} = -3.979 \times 10^{0}$ 1/rad	$C_{m_\alpha} = -9.323 \times 10^{-1}$ 1/rad
$C_{x_{\dot\alpha}} = -1.836 \times 10^{-4}$ s/rad	$C_{z_{\dot\alpha}} = -2.529 \times 10^{-3}$ s/rad	$C_{m_{\dot\alpha}} = -2.135 \times 10^{-3}$ s/rad
$C_{x_q} = -7.019 \times 10^{-4}$ s/rad	$C_{z_q} = -6.229 \times 10^{-3}$ s/rad	$C_{m_q} = -2.093 \times 10^{-2}$ s/rad
$C_{y_\beta} = -1.062 \times 10^{0}$ 1/rad	$C_{l_\beta} = -1.112 \times 10^{-1}$ 1/rad	$C_{n_\beta} = 1.564 \times 10^{-1}$ 1/rad
$C_{y_{\dot\beta}} = -1.167 \times 10^{-3}$ s/rad	$C_{l_{\dot\beta}} = -2.562 \times 10^{-4}$ s/rad	$C_{n_{\dot\beta}} = 9.990 \times 10^{-4}$ s/rad
$C_{y_p} = -3.818 \times 10^{-3}$ s/rad	$C_{l_p} = -2.708 \times 10^{-3}$ s/rad	$C_{n_p} = 9.544 \times 10^{-4}$ s/rad
$C_{y_r} = 2.297 \times 10^{-3}$ s/rad	$C_{l_r} = 1.285 \times 10^{-3}$ s/rad	$C_{n_r} = -8.410 \times 10^{-3}$ s/rad
$\omega_{SP} = 4.613$ rad/s	$\zeta_{SP} = 0.1134$	
$\tau_{P1} = 49.70$ s	$\tau_{P2} = -87.95$ s	
$\omega_{DR} = 2.063$ rad/s	$\zeta_{DR} = 0.09792$	
$\tau_R = 5.893$ s	$\tau_S = 20.12$ s	

Table 5 Handling quality levels at the low condition

Longitudinal	Lateral-directional
ω_{SP}. . .1	ω_{DR}. . .1
ζ_{SP}. . .3	ζ_{DR}. . .1
ζ_P. . .1	τ_R. . .2
	τ_S. . .1

Table 6 Handling quality levels at the design condition

Longitudinal	Lateral-directional
ω_{SP}. . .1	ω_{DR}. . .1
ζ_{SP}. . .3	ζ_{DR}. . .1
ζ_P. . .1	τ_R. . .2
	τ_S. . .1

Table 7 Handling quality levels at the high condition

Longitudinal	Lateral-directional
ω_{SP}. . .1	ω_{DR}. . .1
ζ_{SP}. . .3	ζ_{DR}. . .1
τ_{P1}, τ_{P2}. . .3	τ_R. . .3
	τ_S. . .1

ment arm changes, due to the increasing sweep, and the aerodynamic center aft shift, due to Mach number, cancel one another to an extent. The longitudinal handling-quality levels are affected by the change from the design condition to the high condition, with a level 2.3 average at the high condition.

The roll mode experiences the largest changes of the lateral-directional modes, due to the change from the design condition to the high condition. τ_R experiences a 120% increase. C_{l_p} experiences the largest change of the lateral-directional stability derivatives, 58%. The roll mode change can be expected since C_{l_ρ} depends upon the wing roll moment arm. The lateral-directional handling quality levels are affected by the change from the design condition to the high condition, with a level 1.5 average at the high condition.

Conclusions

One significant conclusion is that variable forward-sweep configurations can have less of a problem with excessive static margins than variable backward-sweep configurations. A 47% reduction in the maximum static margin change was found to occur for a variable forward-sweep configuration relative to a similar variable backward sweep configuration. This is an inherent advantage variable forward sweep possesses relative to variable backward sweep. The advantage is because the aerodynamic center movement due to sweep and Mach number are in opposite directions for variable forward sweep and in the same directions for variable backward sweep.

Most of the stability derivatives that depend upon the wing roll, pitch, and yaw moment arms tend to be affected consistently more by variable forward sweep than the other stability derivatives. These stability derivatives include C_{x_q}, C_{z_q}, C_{m_u}, $C_{m_{\dot{\alpha}}}$, C_{m_q}, C_{l_p}, and C_{n_p}. However, C_{x_q}, C_{z_q}, C_{m_u}, C_{m_α}, and C_{m_q} can be counter-affected by the aerodynamic center shifts due to Mach number. When this occurred, C_{x_u}, C_{x_α}, and C_{z_u}, which do not depend upon the wing moment arms, experienced the largest changes. This indicates the effects from wing location and center of gravity location due to variable forward sweep are more significant than the effects from wing shape due to variable forward sweep.

Although not discussed previously, the steady state trim condition and moments of inertia changes are quite small. The phugoid and roll modes experienced the largest effects of all the characteristic modes. Finally, the average handling-quality levels indicated no drastic changes as the sweep/Mach number condition varied between a lower and upper extreme.

Note carefully that the conclusions of this study are based upon one generic configuration. The flight dynamics of a variable forward-sweep aircraft should no doubt vary with the sweep range, sweep/Mach number profile, pivot location, wing aerodynamic contributions, and wing mass and inertia contributions.

References

[1]Kress, R.W., "Variable Sweep Wing Design," AIAA Paper 80-3043, March 1980.

[2]Polhamus, E.C. and Toll, T.A., "Research Related to Variable Sweep Aircraft Development," NASA TM-83121, May 1981.

[3]Roskam, J., *Airplane Flight Dynamics and Automatic Flight Controls,* Roskam Aviation and Engineering Co., Lawrence, 1979.

[4]Finck, R.D., "USAF Stability and Control DATCOM," Wright-Patterson Air Force Base, Ohio, April 1978.

[5]Sharpes, D.G., "Qualification of the Datcom for Swept Forward Wing Planforms—A Summary of Work to Date," AIAA Paper 83-1836, July 1983.